Characterization and Modeling of the Hydrodynamic Behavior in the Filter-Press-Type FM01-LC Electrochemical Cell by Direct Flow Visualization and Residence Time Distribution

C. Bengoa,† A. Montillet,* P. Legentilhomme, and J. Legrand

Laboratoire de Génie des Procédés, Université de Nantes−Institut Universitaire de Technologie de Saint-Nazaire, B.P. 420, 44606 Saint-Nazaire Cédex, France

In this paper, the hydrodynamics in the FM01-LC electrolyzer is studied by flow visualization and residence time distribution (RTD). Divided and undivided modes are studied by direct visualization, with two injection points. The use of foams instead of turbulence promoters as well as that of electrodes without turbulence promoters is tested. In the membrane-partitioned-mode configurations, radial and axial dispersions are observed. Dispersion is drastically extended in case of empty channel flow. A high-flow asymmetry is generally induced by the flow distributors. RTD is implemented in the whole cell and in the reaction area. The reactor working with a plane plate alone gives a rather constant, low Péclet number, *Pe*, whatever the tested flow rates. The low *Pe* values denote an important axial dispersion. The use of turbulence promoters or foams induces a significant increase of *Pe*, giving plug flow character.

1. Introduction

The continuous progress of electrochemical engineering involves studying and designing more and more efficient electrochemical reactors. Filter-press-type electrochemical reactors are the most common ones used in laboratory and industrial applications. The design evolution of these reactors is due to the need for "zero-effluent" manufacturing processes. The use of three-dimensional electrodes allows one to improve the efficiency of electrochemical processes such as wastewater treatments or electrosynthesis. A great diversity of materials was and is still used and studied as three-dimensional electrodes.[1−15] All of these materials are characterized by a highly active surface that provides high mass transfer.

In this paper, the hydrodynamics in a laboratory-scale commercial filter-press electrolyzer, FM 01-LC from ICI, is studied. The FM 01-LC is abundantly described in the literature:[16] global and local mass transport to electrodes,[17,18] performance of three-dimensional electrodes,[9] pressure drop,[17] and residence time distribution using a simple moment analysis[11] have been studied.

In a previous paper,[13] another laboratory-scale electrolyzer from ElectroCell AB was studied. Following a similar scheme, the present paper first focuses on a direct flow visualization study of the reaction area and then in a model of respectively the global cell and the reaction area thanks to residence time distribution data.

Different configurations of the FM 01-LC are tested respectively in the undivided mode, corresponding to the use of a single fluid, and in the membrane-partitioned mode, when both catholyte and anolyte fluids are processed. The reaction area successively consists of empty channels and channels filled with a classical turbulence promoter or various synthetic foams. In practical works, metallic or RVC foams can be chosen so as to magnify the electrodes surface area. The visualization study is based on the observation of dye dispersion from three injection points respectively located before the cell and in two points of the reaction area itself. Residence time distribution experiments are implemented with salt injection using conductometric probes located in different parts of the reaction area and respectively upstream and downstream from the cell. Experiments are carried out to describe the influence of the inlet system and to investigate the flow establishment in the reaction area. The flow behavior in this cell is compared with that of another commercial filter-press reactor, the ElectroSynCell previously studied.[13]

2. Experimental Details

2.1. Electrochemical Cell. As previously mentioned, the FM 01-LC electrochemical cell has been described in detail in the literature.[11,16−18] The 64-cm^2 projected electrode area cell is a scaled-down version of the FM 21-SP (21 dm^2) developed by ICI. A classical representative unit cell (RUC) consists of a plane plate, the electrode, covered by two plastic nets that act as a turbulence promoter (Figure 1). These plastic nets are located in the spacer, each spacer being located between two gaskets (Figure 1).

In the present work, different RUCs are tested, the configurations of which are summarized in Table 1. The corresponding reaction areas are sketched in Figure 2. In the membrane-partitioned mode (Figure 2) the channel formed by the two electrodes has an interelectrode gap of 6.4 mm. This geometry leads to a hydraulic diameter, d_e, of 11.0 mm. The Reynolds number, *Re*, based on this hydraulic diameter lies between 700 and 2100, and the superficial velocity of the flow, *v*, is varied between 6.4 and 19.3 cm s^{-1}. The empty channel volume is about 41 cm^3.

In the undivided mode (Figure 2), the channel has an interelectrode gap of 11.3 mm, the hydraulic diam-

* To whom correspondence should be addressed. Fax: 33 2 40 17 26 18. E-mail: montill@lgp.univ-nantes.fr.

† Present address: Departamento de Ingeniería Química, Escola Tècnica Superior d'Enginyeria Química, Universitat Rovira i Virgili, Plaza Imperial Tárraco, 1, 43005 Tarragona, Spain.

10.1021/ie9907730 CCC: $19.00
Published on Web 05/27/2000

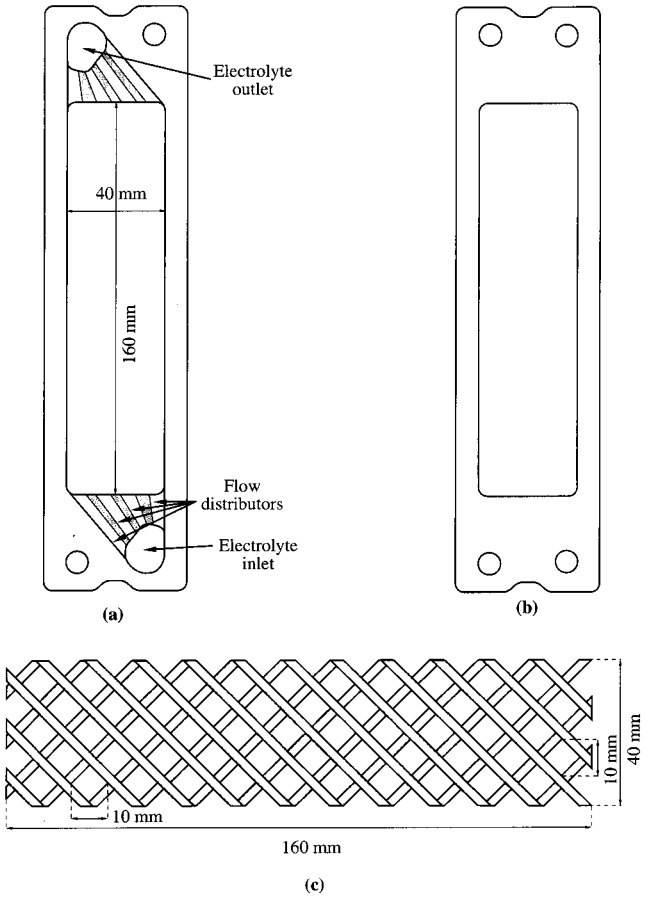

Figure 1. Sketch of a spacer (a), a gasket (b), and a classical turbulence promoter (c) used in the FM 01-LC.

Table 1. Characteristics of the Tested Configurations

name of the configuration	working mode	channel configuration	visualization experiments	RTD experiments
a	membrane-partitioned mode	empty	X	X
b		turbulence promoter	X	X
c		foam(s)	X	X
d	undivided mode	empty		X
e		turbulence promoter		X
f		foam(s)		X
g		turbulence promoter/ foam G60	X	X

eter is 17.6 mm, the Reynolds number lies between 640 and 2800, and the velocity varies between 3.7 and 16.0 cm s^{-1}. The empty channel volume is about 113 cm^3.

The three polyester open-cell foams used have respective grades of 10, 20, and 60 pores/in. A more accurate description of these foams can be found elsewhere.[8,19]

2.2. Flow Visualization. The flow visualization technique used in this work has already been described in our previous works.[13,25] The more interesting techniques to use in this case are the dye injection technique and the electrode-activated pH method. In our previous works, they were both tested. The conclusions from the results obtained with each technique were similar. The dye injection technique is used in this work. It is easy to carry out, a pulse of tracer being injected. The main

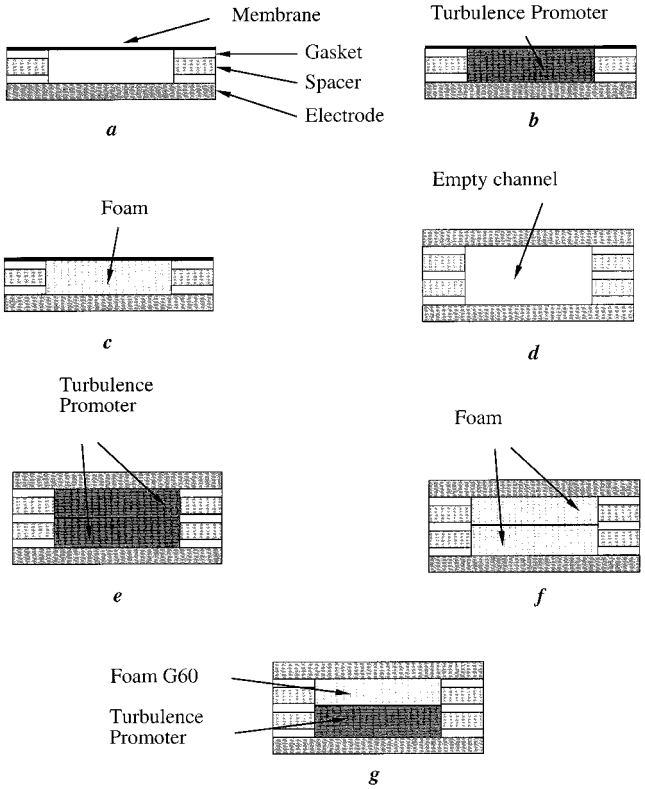

Figure 2. Different configurations studied. Membrane-partitioned mode: a plane plate alone ("a"), a plane plate with turbulence promoters ("b"), and a plane plate with foams ("c"). Undivided mode: a plane plate alone ("d"), a plane plate with turbulence promoters ("e"), a plane plate with foams ("f"), and the last configuration consisting of a plane plate covered with a turbulence promoter and of another one covered with a sheet of foam ("g").

drawback is the possible flow modification due to an eventual overpressure, itself due to the injection mode; molecular diffusion is supposed to be negligible at studied flow rates. With the electrode-activated pH method, a variation of pH is induced at the electrode and then no flow modification occurs, except possible gas evolving if the applied potential is high. The tracer is an analytical indicator; its concentration is uniform and its more colored form is produced where the liquid is affected by the pH modification. The main drawback of this technique is the difficulty in producing a significative color variation in the liquid, and then the tracer must be continuously generated. Bromocresol green with a concentration of 0.4 g dm^{-3} was used as an indicator. The tracer was injected at three different points, the first one being located upstream from the inlet system to visualize its effect on the flow; the last two were located in the left and right parts at the entrance of the reaction area. Figure 3 shows a schematic view of the experimental apparatus. For the purpose of these visualizations, several modifications of the cell were made: one of the metallic frames and one of the electrodes were replaced by a Plexiglas plane plate (246 × 90 × 10 mm). The two injectors are set in this plate, just at the beginning of the reaction area (Figure 3). No modification of geometry and location of flow distributors and of the inlet−outlet system is made from the original cell.

For each injection point and each configuration, six flow rates were tested, respectively: 34, 61, 87, 114, 140, and 167 dm^3 h^{-1}. The flow pattern in the reaction zone was filmed using a video camera connected to a TV

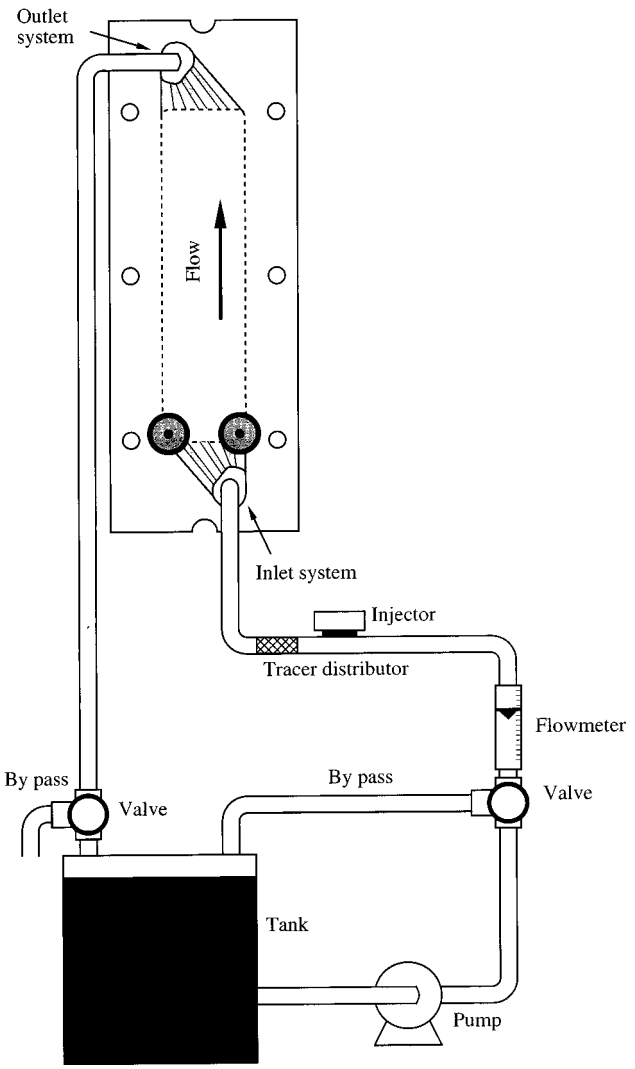

Figure 3. Scheme of the experimental apparatus used during the visualization studies.

monitor and to a videotape recorder. The videotapes were further back-monitored to obtain instantaneous flow pictures. The flow was visualized respectively in the configurations "a", "b", "c", and "g" (Table 1).

2.3. Residence Time Distribution. The residence time distribution (RTD) curves are experimentally determined with a classic conductometric method with two measurement points.[20] The concentration of the injected tracer (an aqueous solution of sodium hydroxide) is measured, as a function of time, with two conductometric cells that consist of two hemicylindrical plates insulated from each other. These cells are connected to two TACUSSEL CD810 variable frequency conductimeters, working at an operating frequency of 1000 Hz to avoid the polarization of the electrodes and to ensure a linear relationship between the conductivity and the tracer concentration. Both concentration signals are sampled using an AOIP SA32 data acquisition device, connected to a personal computer.

To perform a global study first, the conductometric cells are located respectively at the inlet and at the outlet of the electrochemical reactor. The hydraulic circuit is the same as that used during the visualization study; the liquid is not recycled to the tank during RTD experiments. Flow rates are incremented by steps of 9 $dm^3\ h^{-1}$ between 60 and 180 or 260 $dm^3\ h^{-1}$ according to the tested configuration. All configurations ("a", "b", "c", "d", "e", "f", and "g") were tested in the global modeling of the electrochemical cell.

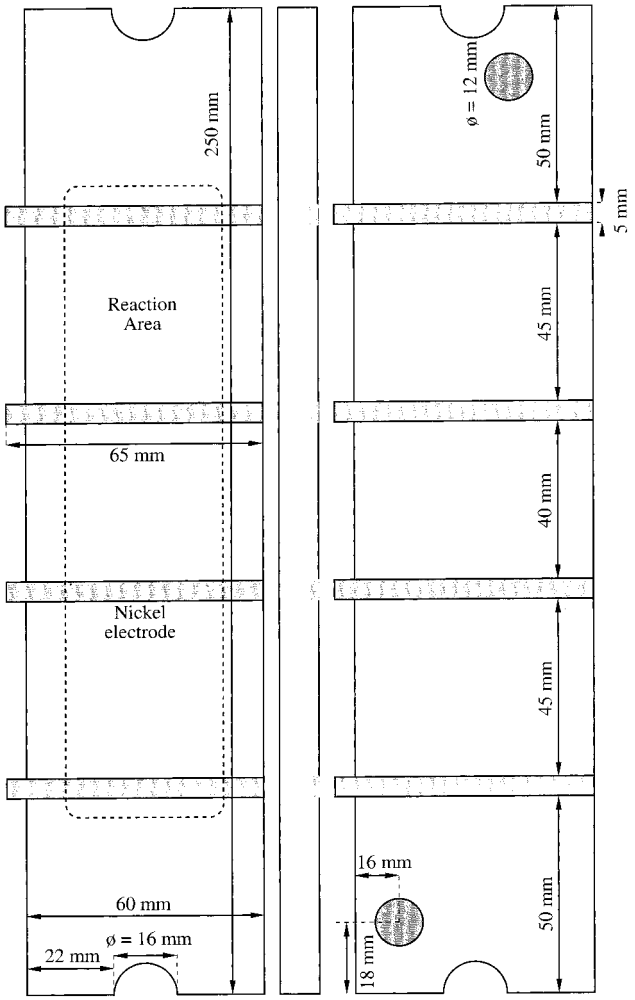

Figure 4. Scheme of the modified plane plates used during the reaction area residence time distribution studies.

In the reaction area of configuration "e", RTD curves are experimentally determined with a set of four probes, distributed along the reaction zone of the electrochemical cell. Each probe consists of two nickel strips, 65 × 5 mm, inserted in two Plexiglas plane plates (250 × 90 × 10 mm), replacing the original metallic electrodes. The distance between the beginning of each conductometric probe and the leading edge of the plates is respectively 50, 95, 135, and 180 mm (Figure 4). The nickel conductometric electrodes are designed in such a way as to cover the entire width of the reaction area. As for the visualization study, the geometry and location of flow distributors and inlet−outlet system of the original cell are not modified.

3. Flow Modeling

3.1. Experimental Curves. As a two-point measurement method is implemented, inlet, $X(t)$, and outlet, $Y(t)$, tracer concentration curves are analyzed by curve fitting in the time domain.[21−23] This method is considered the best way to determine the parameters of a given flow model using residence time measurements.[21] The experimental response (outlet curve) is compared with the calculated one, $Y^*(t)$, using the inlet curve and the transfer function of the model, $F(i,\omega)$, given by

$$F(i\omega) = \frac{\int_0^{2T} \exp(-i\omega)\, Y^*(t)\, \mathrm{d}t}{\int_0^{2T} \exp(-i\omega)\, X(t)\, \mathrm{d}t} \quad (1)$$

The parameters of the model are optimized by minimization of the root-mean-square error, E_r, between the calculated and experimental outlet signals using the Rosenbroock algorithm,[24]

$$E_r = \left[\frac{\int_0^{2T} (Y(t) - Y^*(t))^2\, \mathrm{d}t}{\int_0^{2T} (Y(t))^2\, \mathrm{d}t}\right]^{1/2} \quad (2)$$

where $2T$ is the time allowing the tail of the response signal $Y(t)$ to vanish.

3.2. Global Modeling. The dispersed plug flow (DPF) model was used to describe the global behavior of the cell. This model has been extensively used to describe the flow in reactors filled with porous media.[11,20,25] Its main advantage lies in its simple use for mass-transfer and reactor performance calculations.

Assuming that the lateral dispersion is negligible with respect to the longitudinal dispersion and that no chemical reaction occurs, the concentration of the injected tracer is given as a function of time, t, and axial position, z, by the axial dispersed plug flow model:

$$\frac{\partial C}{\partial t} = D_{ax}\frac{\partial^2 C}{\partial x^2} - \frac{U_0}{\epsilon}\frac{\partial C}{\partial x} \quad (3)$$

The transfer function of the DPF model in the Fourier domain is given by[22]

$$F(i\omega) = \exp\left\{\frac{Pe}{2}\left[1 - \left(1 + \frac{4}{Pe}\tau_1 i\omega\right)^{1/2}\right]\right\} \quad (4)$$

where the Péclet number, Pe, is defined by

$$Pe = \frac{U_0}{\epsilon}\frac{L}{D_{ax}} \quad (5)$$

U_0, ϵ, and L are, respectively, the superficial velocity, the cell void fraction, and its length. The Péclet number and the mean residence time, τ_1, are the two optimized parameters of the DPF model.

3.3. Reaction Area and Inlet−Outlet System Modeling. To model the reaction area, two probes were located at the ends of the plates, delimiting the reaction area. The DPF model is used to model the reaction area.

Because of the geometrical structure of the inlet system, it was impossible to locate two identical conductometric probes upstream and downstream from it. To overcome this problem, we attempted to model the inlet−outlet system from the global model of the electrochemical cell and from that of the reaction zone. For this goal, the whole electrochemical cell is described with a series (DPFCSTR) of a DPF model and a cascade of identical volume CSTRs in series instead of a single DPF model (see section 3.2). The DPF corresponds to the flow in the reaction area and the CSTRs to the flow in the inlet−outlet system. The transfer function of DPFCSTR in the Fourier domain is given by

$$F(i\omega) = \exp\left\{\frac{Pe}{2}\left[1 - \left(1 + \frac{4}{Pe}\tau_1 i\omega\right)^{1/2}\right]\right\}\left\{\frac{1}{(1 + \tau_2 i\omega)^J}\right\} \quad (6)$$

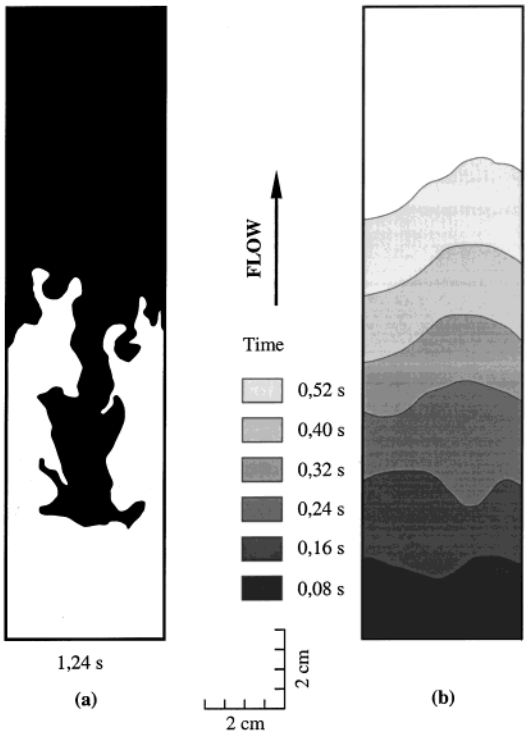

Figure 5. Visualization by dye injection before the inlet system of the cell working in the membrane-partitioned mode: plane plate alone (configuration "a")) with $Q_V = 34$ l h^{-1} (a) and turbulence promoter (configuration "b") with $Q_V = 114$ l h^{-1} (b).

The parameters Pe and τ_1, corresponding to the reaction area, are fixed to the values obtained during the reaction area modeling. The optimized parameters, corresponding to the inlet−outlet system, are τ_2, the mean residence time in the cascade of CSTRs in series, and J, the number of CSTRs.

4. Flow Visualization

4.1. Dye Injection before the Inlet System of the Cell. In the membrane-partitioned mode, with configuration "a" (plane plate alone), the flow is perturbed by the inlet−outlet system of the cell; an example of flow visualization is given in Figure 5 a. The flow pattern is not uniform. Recirculations at the entrance of the reaction area are detected; both axial and radial dispersions are also observed. Both behaviors, recirculation and dispersion, induce a thorough stirring of the tracer before it reaches the outlet system of the cell. Moreover, the velocity of the flow is higher in both lateral zones of the reaction area.

The flow pattern is drastically different when turbulence promoters are used (configuration "b", Figure 5b); the flow is quite uniform along the reaction area. Axial dispersion is observed at the beginning of the reaction area. It seems that the turbulence promoter is efficient, giving the flow a turbulent-like velocity profile, hence, a plug flow character. Along the reaction area, the velocity in the right-hand part seems to increase compared with the velocity in the left-hand part, which may be due to flow distributors asymmetry.

In the membrane-partitioned mode, the asymmetric character of the axial velocity distribution is increased when the flat plate is covered with G60 foams (configuration "c") instead of turbulence promoters.

With configuration "g", in the undivided mode, an intermediate flow pattern is developed between that

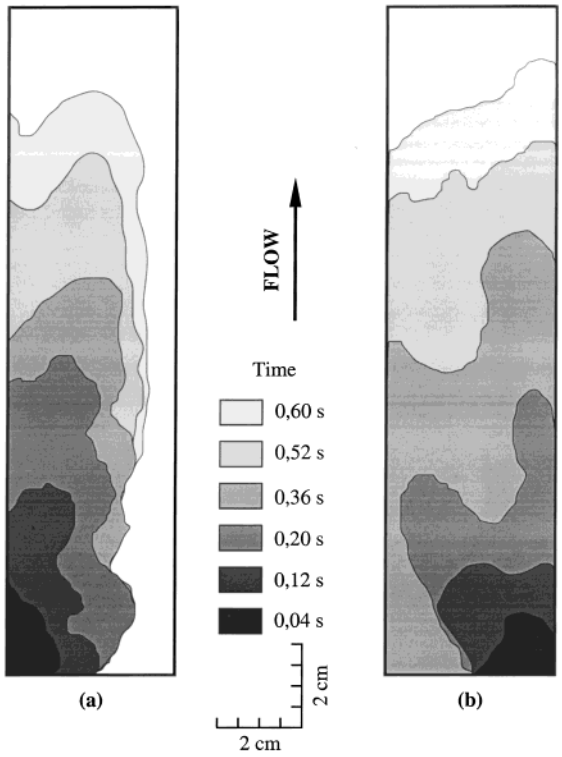

Figure 6. Visualization of the reactor in the membrane-partitioned mode: turbulence promoter (configuration "b") with Q_V = 114 l h^{-1}: dye injection in the left part of the cell (a) and dye injection in the right part of the cell (b).

observed with configuration "b" and that observed with configuration "c". It still corresponds to an asymmetric distribution of the axial flow velocity.

4.2. Dye Injection in the Reaction Area. In the membrane-partitioned mode, with plane plate alone (configuration "d"), important recirculation effects are noticed, as previously observed with a tracer injection before the inlet system. Both lateral and axial dispersions are detected. These dispersion phenomena are slightly more pronounced in the left zone of the active area.

With the use of turbulence promoters, configuration "e" (Figure 6, left injector (a), right injector (b)), both radial and axial dispersions are observed from injections at the left and right tracer ports. However, lateral dispersion is more important in the right part of the cell. This character induces a high asymmetry of the flow pattern.

With G60 foams, configuration "f", both radial and axial dispersion phenomena are less important. The latter configuration involves the lowest dispersion. An asymmetry of the flow behavior from the two tracer injectors is also observed, still corresponding to an increase of the axial velocity in the right part of the reaction area.

Finally, in the undivided mode, with a plane plate covered with a turbulence promoter and the other one covered with a G60 foam (configuration "g"), as previously observed with the same configuration when an injection is made before the inlet system, the flow behavior is intermediate between those observed in configurations "e" and "f". The flow behavior, in this case, is very similar to that previously visualized with the same configuration in the ElectroSynCell electrolyzer.[13]

Table 2. Global Modeling with the DPF Model: Mean Values of the Péclet Number, *Pe*, and the Corresponding Values of the Standard Deviation

	membrane partitioned mode		undivided mode	
tested configuration	mean Péclet number	standard deviation	mean Péclet number	standard deviation
plane plate alone	17	±4	18	±3
turbulence promoter	100	±18	63	±5
G10 foam	134	±41	80	±9
G20 foam	181	±61	99	±16
G60 foam	169	±38	166	±49
turbulence promoter + G60 foam			22	±4

5. RTD Results

5.1. Global Modeling in the Membrane-Partitioned Mode. In this first global modeling study, the DPF model was used for the five respective configurations: a plane plate alone (configuration "a"), a plane plate with a turbulence promoter (configuration "b"), and a plane plate successively covered with a sheet of grade G10, G20, and G60 foams (configuration "c"). For each studied configuration, the values of the observed error, E_r, range between 1% and 5%, thereby demonstrating the reliability of the DPF model. The range of Q_V values covers the whole hydrodynamic domain suggested by the manufacturer (ICI). The mean values of the Péclet number, *Pe*, with their corresponding standard deviations, σ, are summarized in Table 2.

When a plane plate alone is used, the Péclet number is quite constant against the volumetric flow rate, and the small values of this parameter indicate that the flow does not exhibit a plug character. The average Péclet number is 17.2 ± 3.5. This behavior confirms the analysis of the flow visualization which shows important axial and radial dispersion phenomena. The values of the Péclet number obtained for this configuration are in agreement with those presented by Trinidad and Walsh[11] in the FM 01-LC reactor.

When a classical turbulence promoter is used, the Péclet number is quite constant, but the average value is higher, 100 ± 18, than that in the previous configuration, and emphasizes a plug flow behavior. This result also confirms the analysis of the flow visualization. The values of the Péclet number, *Pe*, do not agree with those presented by Trinidad and Walsh,[11] who found Péclet numbers, *Pe*, of about 18. In their study,[11] the difference with results obtained with a plane plate alone does not exceed 30%. In our work, the ratio of the mean Péclet numbers calculated for the two configurations is about 5. The value of this ratio, obtained in a previous study based on the same experimental method, but with the ElectroSynCell, is 2.[8] The discrepancy between our results and those of Trinidad and Walsh[11] may be explained by the difference in the experimental methods used. In particular, Trinidad and Walsh[11] used a single-measurement-point method.

The higher average Péclet number, 169 ± 38, obtained for the configuration "g" using a G60 foam, indicates a significant plug flow character. The weak dispersion observed during flow visualization is emphasized by these results. The Péclet number value, *Pe*, is not uniform and increases with the volumetric flow rate,

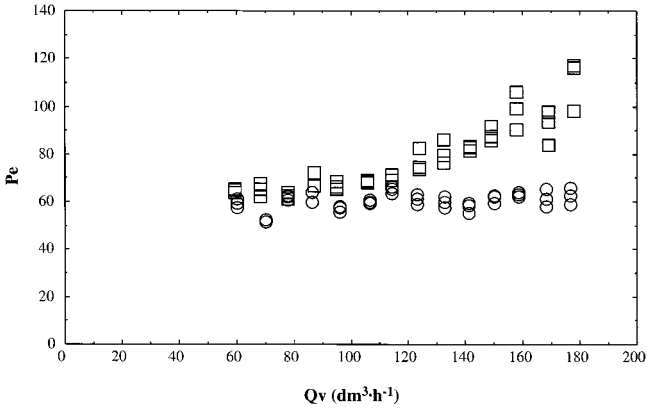

Figure 7. Plot of *Pe* versus Q_V for the different zone modelings (configuration "e"): (○) global ($Pe = 63 \pm 5$) and (□) reaction area ($Pe = 80 \pm 15$).

Q_V. However, a variation of *Pe* when its value is higher than 100 has no particular physical meaning.[26]

The results obtained with the three different foams (G10, G20, and G60) are very similar. Respective average Péclet numbers, 133 ± 41, 181 ± 61, and 169 ± 38, are obtained. Thus, no particular difference between the flow behavior observed with the three foams can be distinguished. The interest of using grade G60 rather than G10 or G20 as a three-dimensional electrode is based on the higher value of its specific surface area.

5.2. Global Modeling in the Undivided Mode. Six configurations are tested: plane plates alone (configuration "d"), plane plates with turbulence promoters (configuration "e"), plane plates respectively covered with sheets of G10, G20, and G60 foams (configurations "f"), and finally, a plane plate covered with a turbulence promoter and the other one covered with a sheet of G60 foam (configuration "g"). The mean values of the Péclet number, *Pe*, with their corresponding standard deviations, σ, are summarized in Table 2.

In general, the data obtained in the undivided mode show similar behaviors as those observed in the membrane-partitioned mode. The Péclet number values are quite similar for each configuration. No significant difference is noted, except for mean values of *Pe* obtained in the undivided mode which are characterized by lower values of their standard deviation.

The behavior obtained with the configuration "g" (turbulence promoter/G60 foam) is quite unexpected. The obtained values of the Péclet number are very low; they are of the same order of magnitude as those obtained with a plane plate alone. The same phenomenon was observed in the ElectroSynCell by Montillet et al.,[8] but the *Pe* values obtained with the foam were slightly higher than those observed with a plane plate alone.

5.3. Reaction Area Modeling. Reaction area modeling was performed thanks to two probes respectively located at the inlet and at the outlet of the reaction zone. The single configuration "e" (undivided mode with turbulence promoters) was studied. *Pe* values are plotted in Figure 7 as a function of the volumetric flow rate, Q_V. In this configuration, the flow exhibits a higher plug character than that in the whole cell, when the flow rate value is higher than 120 $dm^3\ h^{-1}$.

5.4. Inlet−Outlet System Modeling. The DPFC-STR model is tested for the modeling of the same "e" configuration (without membrane/turbulence promoters). The average number of reactors in the series modeling the inlet−outlet system is independent of Q_V and equal to 4 ± 1. This value is in complete agreement with that presented by Montillet et al.[8] for the ElectroSynCell reactor. The low number of reactors is the consequence of a high-dispersion phenomenon, which induces high mixing before the entrance of the reaction area and leads to a rather homogeneous concentration of chemical species in the entrance section of the reaction area.

Table 3. Modeling the Reaction Area: Mean Values of Péclet Number, *Pe*, Axial Dispersion Coefficient Divided by Kinematic Viscosity, and Corresponding Values of the Standard Deviation; Configuration "e" (Undivided Mode/Turbulence Promoters); DPF Model

electrodes distances (mm)	mean Péclet number	D_{ax}/ν
145	80 ± 15	233 ± 30
95	52 ± 12	239 ± 32
50	35 ± 7	187 ± 37

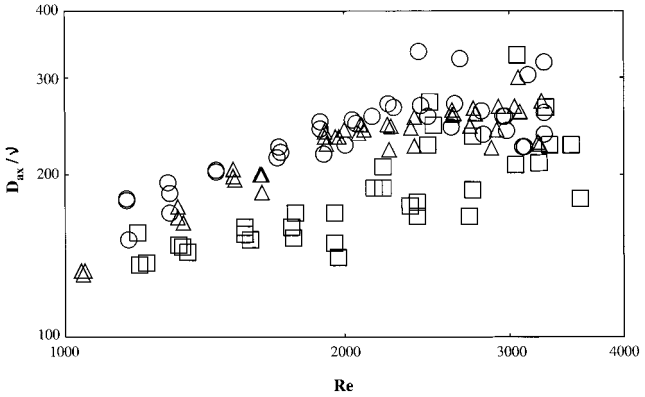

Figure 8. Plot of the axial dispersion coefficient, D_{ax}, calculated in different sections of the reaction area versus the Reynolds number, *Re*. Respective lengths tested (from the entrance): 130 (△), 85 (○), and 45 mm (□).

5.5. Local Study of the Reaction Zone. In the final part of this work, the DPF model was used to study the different sections bounded by the probes installed in the reaction area. The tested configuration is still the "e" one. The mean values of the Péclet number are summarized in Table 3. On one hand, *Pe* increases with Q_V in each studied section. On the other hand, *Pe* also increases with the length of the reaction area section, denoting a nonestablished flow regime with an increasing plug flow character along the reaction area.

Figure 8 shows the experimental values of the axial dispersion coefficient divided by the kinematic viscosity, D_{ax}/ν, against the Reynolds number, *Re*. The use of D_{ax}/ν gives a more precise overview of the study because it is a dimensionless parameter, independent of the velocity and of the length between the electrodes. Mean values of axial dispersion coefficients are summarized in Table 3. For each section, D_{ax} increases with the Reynolds number, but the most important point is that the axial dispersion coefficient is not constant along the reaction area; it increases in the entrance part of the reaction area (50 mm in length) and seems to be constant in the remaining part. These results prove that the flow is not totally established in the beginning part of the reaction zone. The same behavior was observed by Bengoa et al.[13] for the ElectroSynCell electrolyzer, where the flow was shown not to be fully developed throughout the reaction area and confirms the results presented by Brown et

al.,[18] where a slight variation of the local mass-transfer coefficient was observed along the reaction area.

6. Conclusions

This work aimed at completing previous studies devoted to flow characterization in commercially available filter-press-type electrochemical reactors. Previously described flow patterns in the ElectroSynCell are globally confirmed in this cell, that is, the quasi-plug-flow character with turbulence promoters or foams (in the membrane-partitioned mode) and the importance of the mixing in the inlet system of the cell. However, a quasi-systematic phenomenon is observed which is an asymmetric distribution of the tracer along the width of the reaction area. It is analyzed as a consequence of a maldistribution of the velocity because of the inlet system geometry. This is a particularity of FM 01-LC cell conception which was previously observed by Brown et al.[18] in a study of the local mass-transfer coefficients.

The flow in the FM 01-LC cell is rather easy to model as simple classical models are shown to be suitable and using foams is not damaging the hydrodynamics compared to the use of the plastic net. From an electrochemical engineering point of view, apart from the configurations "a" and "d" (empty channels), which are studied with the objective of making a more academic comparison with other configurations, all the tested configurations can be used, depending on the involved reaction and the kind of application. A systematic use of an inert foam or an active one rather than a classical turbulence promoter cannot be a general conclusion, as it can be deduced from our experiments. The choice of using or not metallic or RVC foams depends on the involved reaction, on the potential, or on the current density to apply. It also depends on the electrode material to be used, thus on the availability of the corresponding foams. The choice of the working mode (divided/undivided) is also concerned with the involved reaction.

Acknowledgment

Christophe Bengoa thanks the Direcció General de Recerca of the Generalitat de Catalunya for financially supporting this research. The authors thank the Direction des Etudes et Recherches d'Electricité de France for supplying the FM 01-LC cell.

Notations

D_{ax} = axial dispersion coefficient ($m^2\ s^{-1}$)
d_c = depth of the channel (m)
d_e = hydraulic diameter of the channel, $d_e = 2w_cd_c/(w_c + d_c)$ (m)
E_r = mean root square error (%)
$F(i\omega)$ = transfer function in the Fourier domain
J = number of continuous stirred tank reactors in the cascade
L = length between the two probes (m)
Pe = Péclet number, $Pe = U_0L/\epsilon D_{ax}$
Q_V = volumetric flow rate ($m^3\ s^{-1}$)
Re = Reynolds number, $Re = d_eU_0/\nu$
U_0 = mean superficial velocity ($m\ s^{-1}$)
w_c = width of the channel (m)
v = flow linear velocity ($m\ s^{-1}$)
$X(t)$ = experimental signal at the inlet of the studied section
$Y(t)$ = experimental signal at the outlet of the studied section
$Y^*(t)$ = calculated signal at the outlet of the studied section

Greek Letters

ϵ = porosity
σ = standard deviation
ν = kinematic viscosity ($m^2\ s^{-1}$)
τ_1 = mean residence time in the PDF model (s)
τ_2 = mean residence time in the cascade of CSTRs in series model (s)

Literature Cited

(1) Marracino, J. M.; Coeuret, F.; Langlois, S. A First Investigation of Flow-Through Porous Electrodes Made of Metallic Felts or Foams. *Electrochim. Acta* **1987**, *32*, 1303.

(2) Carta, R.; Palmas, S.; Polcaro, A. M.; Tola, G. Behaviour of a Carbon Felt Flow by Electrodes. Part I: Mass Transfer Characteristics. *J. Appl. Electrochem.* **1991**, *21*, 793.

(3) Pletcher, P.; Whyte, I.; Walsh, F. C.; Millington, J. P. Reticulated Vitreous Carbon Cathodes for Metal Ion Removal from Process Streams. Part I: Mass Transport Study. *J. Appl. Electrochem.* **1991**, *21*, 659.

(4) Pletcher, P.; Whyte, I.; Walsh, F. C.; Millington, J. P. Reticulated Vitreous Carbon Cathodes for Metal Ion Removal from Process Streams. Part II: Removal of Copper(II) from Acid Sulphate Media. *J. Appl. Electrochem.* **1991**, *21*, 667.

(5) Walsh, F. C.; Pletcher, P.; Whyte, I.; Millington, J. P. Electrolytic Removal of Cupric Ions from Dilute Liquors Using Reticulated Vitreous Carbon Cathodes. *J. Chem. Technol. Biotechnol.* **1992**, *55*, 147.

(6) Pletcher, P.; Whyte, I.; Walsh, F. C.; Millington, J. P. Reticulated Vitreous Carbon Cathodes for Metal Ion Removal Process Streams. Part III: Studies of a Single Pass Reactor. *J. Appl. Electrochem.* **1993**, *23*, 82.

(7) Qi, J.; Savinell, R. F. Analysis of Flow-through Porous Electrode Cell with Homogeneous Chemical Reactions: Applications to Bromide Oxidation in Brine Solutions. *J. Appl. Electrochem.* **1993**, *23*, 873.

(8) Montillet, A.; Comiti, J.; Legrand, J. Application of Metallic Foams in Electrochemical Reactors of Filter-Press Type. Part I: Flow Characterization. *J. Appl. Electrochem.* **1993**, *23*, 1045.

(9) Brown, C. J.; Pletcher, D.; Walsh, F. C.; Hammond, J. K.; Robinson, D. Studies of Three-Dimensional electrodes in the FM01-LC Laboratory Electrolyser. *J. Appl. Electrochem.* **1994**, *24*, 95.

(10) Montillet, A.; Comiti, J.; Legrand, J. Application of Metallic Foams in Electrochemical Reactors of the Filter-Press Type. Part II: Mass Transfer Performance. *J. Appl. Electrochem.* **1994**, *24*, 384.

(11) Trinidad, P.; Walsh, F. C. Hydrodynamic Behaviour of the FM01-LC Reactor. *Electrochim. Acta* **1996**, *41*, 493.

(12) Cognet, P.; Berlan, J.; Lacoste, G.; Fabre, P. L.; Jud, J. M. Application of Metallic Foams in an Electrochemical Pulsed Flow Reactor. Part II: Oxidation of Benzyl Alcohol. *J. Appl. Electrochem.* **1996**, *26*, 631.

(13) Bengoa, C.; Montillet, A.; Legentilhomme, P.; Legrand, J. Flow Visualization and Modelling of a Filter-Press Type Electrochemical Reactor. *J. Appl. Electrochem.* **1997**, *27*, 1313.

(14) Szánto, D.; Trinidad, P.; Walsh, F. C. Evaluation of Carbon Electrodes and Electrosynthesis of Coumestan and Catecholamine Derivatives in the FM01-LC Electrolyser. *J. Appl. Electrochem.* **1998**, *28*, 251.

(15) González García, J.; Montiel, V.; Aldaz, A. Hydrodynamic Behavior of a Filter-Press Electrochemical Reactor with Carbon Felt as a Three-Dimensional Electrode. *Ind. Eng. Chem. Res.* **1998**, *37*, 4501.

(16) Walsh, F.; Robinson, D. Electrochemical Filter-Press Reactors —Technology Designed for Versatility and Efficiency. *Electrochem. Soc. Interface* **1998**, Summer, 40.

(17) Brown, C. J.; Pletcher, D.; Walsh, F. C.; Hammond, J. K.; Robinson, D. Studies of Space-Average Mass Transport in the FM01-LC Laboratory Electrolyser. *J. Appl. Electrochem.* **1993**, *23*, 38.

(18) Brown, C. J.; Pletcher, D.; Walsh, F. C.; Hammond, J. K.; Robinson, D. Local Mass Transport Effects in the FM01 Laboratory Electrolyser. *J. Appl. Electrochem.* **1992**, *22*, 613.

(19) Montillet, A. Fiabilité de la Détermination de Paramètres Structuraux de Mousses Synthétiques à Partir de Mesures de Chute de Pression. *Récents Progrès Génie Procédés* **1995**, *9* (41), 125.

(20) Legentilhomme, P.; Legrand, J.; Comiti, J. Axial Dispersion in Electrolyte Flow through Anisotropic Packed Beds. *J. Appl. Electrochem*. **1989**, *19*, 263.

(21) Fahim, M. A.; Wakao, N. Parameter Estimation from Tracer Response Measurements. *Chem. Eng. J*. **1982**, *25*, 1.

(22) Wakao, N.; Kaguei, S. *Heat Transfer in Packed Beds*; Gordon and Breach Science Publishers: New York, 1992.

(23) Clements, W. C. A Note on Determination of the Parameters of the Longitudinal Dispersion Model from Experimental Data. *Chem. Eng. Sci.* **1969**, *24*, 957.

(24) Beveridge, G. S. G.; Schechter, R. S. *Optimization: Theory and Practice*; McGraw-Hill: New York, 1992.

(25) Montillet, A.; Legrand, J.; Comiti, J.; Letord, M. M.; Jud, J. M. Use of Metallic Foams in Electrochemical Reactors of Filter-Press Type: Mass Transfer and Flow Visualization. In *Electrochemical Engineering and Energy*; Plenum Press: New York, 1994; p 81.

(26) Villermaux, J. *Génie de la Réaction Chimique. Conception et Fonctionnement des Réacteurs*; Technique et Documentation; Lavoisier: Paris, 1984.

Received for review October 25, 1999
Revised manuscript received February 23, 2000
Accepted March 1, 2000

IE9907730